Biocompatibility of Materials Implanted into the Subretinal Space of Yucatan Pigs

Sandra R. Montezuma,[1] *John Loewenstein,*[1] *Carmen Scholz,*[2] *and Joseph F. Rizzo, III*[1,3]

Purpose. To assess the biocompatibility of materials for possible use in subretinal prostheses.

Methods. Strips (0.5 × 5 mm; 10-μm thick) of either plain poly(imide) or poly(imide) coated with amorphous aluminum oxide (AAO), amorphous carbon (AC), parylene, poly(vinyl pyrrolidone) (PVP), or poly(ethylene glycol) (PEG) were each implanted into the subretinal space of four Yucatan miniature pigs. Two types of control surgery without implantation were performed in four other animals. Electroretinograms (ERGs) were performed before and after surgery. All animals were euthanatized 3 months after surgery, and histologic slides of the retina were assessed for 15 criteria. Paired, two-tailed Student's *t*-tests were used for statistical analyses.

Results. Across all animals, the mean amplitude of the ERG b-wave did not differ from baseline after 3 months. In implanted animals, the histologic analyses revealed that (1) all the implanted materials produced abnormalities that were significantly greater than in the control subjects; (2) overall, PEG, parylene, and PVP produced less histologic disruption than the other three materials; (3) parylene and PEG did not differ significantly from the control in disturbing retinal anatomy; (4) only PI and AAO produced RPE alterations that were significantly greater than in control subjects; and (5) AAO and PI produced a significantly greater degree of peri-implant cellular responses than did the other materials.

Conclusions. All implants produced some alteration of the retina, but there were clear differences among the materials in the degree to which their presence disturbed the normal anatomy of the retina or RPE or incited tissue reactions around the implant. (*Invest Ophthalmol Vis Sci.* 2006;47:3514–3522) DOI:10.1167/iovs.06-0106

Our group is developing a retinal prosthesis to restore vision to patients with disease of the outer retina, especially retinitis pigmentosa and age-related macular degeneration.[1–4] An acceptable level of biocompatibility must be demonstrated for the materials used in a prosthesis before long-term implantation in humans. In this regard, we use the term "biocompatible" in the broadest sense, which should include consideration of any inflammation, "rejection," or tissue damage that result from reactions to (1) implant materials, (2) surgical disruption of the eye, and (3) chemical reactions induced by the electrical activity of the device.

In this study, we report on the biocompatibility of six materials that are suitable candidates as a substrate for microfabrication and/or electrical insulators that could be used in a retinal prosthesis. We have attempted to isolate the biological responses to the materials themselves by minimizing surgical trauma and by not introducing electrical activity. We placed the materials in contact with the retina to maximize our ability to determine whether there would be adverse effects on the retina, which contains the neurons that the prosthesis would be stimulating.

The biocompatibility of materials suitable for a retinal prosthesis has been studied previously, both for epiretinal and subretinal implantation.[5–11] (See the Discussion section for a detailed analysis of these earlier studies.) Our study differs from these others in that we (1) implanted only one material in each animal, which removes a potentially confounding factor in judging biocompatibility; (2) surveyed the responses to a selection of (i.e., six) prosthetically relevant materials (Table 1) across a relatively large number of animals; (3) assessed a large number (i.e., 15) of histologic criteria; (4) obtained a large representation of histology (i.e., 100 slides for each material); (5) quantified and statistically compared the histologic results; and (6) performed control experiments.

Materials and Methods

Twenty-eight Yucatan miniature pigs (20 kg) were studied. Our protocol was approved by the animal care committee of the Massachusetts Institute of Technology. All animals were treated in accordance with the ARVO Statement for the Use of Animals in Ophthalmic and Vision Research.

In advance of surgery, an electroretinogram (ERG) was obtained through a pharmacologically dilated pupil by placing a recording electrode (ERG-JET; LKC Technologies, Gaithersburg, MD) on the cornea. The common and ground references were on an ear. The retina was stimulated with a photostimulator (PS22 x, Mini Ganzfeld, model PSD22D; Grass-Telefactor, West Warwick, RI) positioned 2 cm from the cornea. The photostimulator's flash intensity setting was 2 (equal to 2.75 lumen s/ft^2 for a 10-μs flash), and the flash frequency was 2 Hz. The endpoint parameter was b-wave amplitude, measured from the negative peak of the a-wave to the positive peak of the b-wave. Each trial consisted of 100 consecutive, computer-averaged stimulations. The results of two trials (i.e., total of 200 stimulations) were averaged. Noise recordings were obtained with identical methods, except that a light or electrical stimulus was not delivered. Ambient illumination was 480 lux (i.e., photopic condition).

For surgery, animals were induced with an intramuscular injection of tiletamine (4 mg/kg), xylazine (2.2 mg/kg), and atropine (0.04 mg/kg) and then were maintained under sufficient anesthesia with 1% to 2% isoflurane inhalation. The pupil was dilated with 0.8% tropicamide, 5.0% phenylephrine hydrochloride, and 1% atropine sulfate. A three-port pars plana vitrectomy was performed with a vitrector (Storz Premiere, model DP2072; Bausch & Lomb, Tampa, FL). After the vitrectomy, a local retinal detachment was created in the superior–nasal retina of the right eye by subretinal injection of balanced saline

From the [1]Massachusetts Eye and Ear Infirmary and the Department of Ophthalmology, Harvard Medical School, Boston, Massachusetts; the [2]Department of Chemical Engineering, University of Alabama, Huntsville, Alabama; and [3]The Center for Innovative Visual Rehabilitation, VA Medical Center, Boston, Massachusetts.

Supported by the Department of Veterans Administration and the Lions Club of Massachusetts.

Submitted for publication January 31, 2006; accepted May 31, 2006.

Disclosure: **S.R. Montezuma**, None; **J. Loewenstein**, None; **C. Scholz**, None; **J.F. Rizzo, III**, None

The publication costs of this article were defrayed in part by page charge payment. This article must therefore be marked "*advertisement*" in accordance with 18 U.S.C. §1734 solely to indicate this fact.

Corresponding author: Joseph F. Rizzo, III, Massachusetts Eye and Ear Infirmary, 243 Charles Street, Boston, MA 02114; joseph_rizzo@meei.harvard.edu.

Investigative Ophthalmology & Visual Science, August 2006, Vol. 47, No. 8

TABLE 1. Characteristics for Each Implanted Material

Material	Thickness	Method of Attachment to Polyimide
Polyimide	10 μm	
Parylene	2 μm	Physico-adsorption deposition
Amorphous aluminum oxide	175 nm	Argon ion beam chemical vapor deposition
Amorphous carbon	60 nm	Pulsed laser ablation of a graphite target using a custom-built Neocera instrument.
Poly(vinyl pyrolidone)	Indeterminate	Physico-adsorption out of a 25% polymer solution in isopropanol
Poly(ethylene glycol)	Monolayer	Chemico-sorption by depositing a gold layer onto the PI-film

Polyimide was the only substrate material. The other materials were applied as coatings onto the 10-μm-thick polyimide strips.

solution via a Lambert cannula. The surgery was stopped at this point in two animals, which served as nonsurgical control subjects. In the other two control animals, a single strip of PI was inserted through the retinotomy and into the subretinal space, where it was held for 2 minutes and then removed. In the other 24 animals, a single strip of one of six materials (Table 1) was implanted in the subretinal space through the retinotomy with a custom-designed insertor (Fig. 1). After surgery, 0.5 mL dexamethasone (0.4 mg/mL) was injected into the subconjunctival space, dexamethasone/tobramycin eye drops were administered three times daily for 1 week, and subcutaneous injections of buprenorphine (0.008 mg/kg) were given for pain control.

After surgery, ERGs were obtained at 1 week and 1, 2, and 3 months. Fundus photography was performed monthly. Animals were killed at 3 months, and histologic slides of the retinas were prepared after immersion in Karnowski's fixative. The tissue was embedded in glycol methacrylate (Historesin; LKB Pharmacia Diagnostics AB, Stockholm, Sweden), and 2-μm sections were cut and stained with hematoxylin-eosin.

Implanted Materials

One of six implants, each as 0.5 $\times$ 5.0-mm strips with a 10-μm substrate thickness, was implanted in an animal (Table 1). Each implant type was received by four animals; hence, 24 animals underwent implantation. PI was used as a control substrate; all other materials were deposited onto the PI as coatings.

The purity of all materials was optimized in the following ways. PI was purchased as a prepolymer (product PI-2611; HD Microsystems, Parlin, NJ), and was certified to have a total metals content of less than 10 parts per million (PPM) and a total chloride of less than 1 PPM. The PI was polymerized by curing under nitrogen. All substrates were prepared in a class 100 microfabrication clean room at the Cornell Nanofabrication Facility (Ithaca, NY), and all substrates were cleaned with HPLC-grade acetone before a coating was applied.

PEG and PVP were purchased as polymers and used without further purification. The PEG was deposited onto a PI substrate out of a solvent mixture of dioxolane water in a 90:10 ratio. The PVP was deposited onto a PI substrate out of isopropanol solvent (≥99% pure). The PVP (Sigma-Aldrich, St. Louis, MO) was not medical grade, but due to the macromolecular nature of this compound, any contamination from the polymer synthesis should be negligible. For AC and AAO, purity was assured to be at the 99.9% level because of the processes used for the depositions. The depositions were performed in a vacuum, within a chamber that was evacuated at the beginning of each procedure. For AC, a 99.9% graphite target was used. For AAO, a pure aluminum target was used, and the sputter deposition was performed in pure oxygen. The parylene dimer was purchased from SCS Cookson (Indianapolis, IN), with certification of purity.

FIGURE 1. Custom-made device used to insert implants through a retinotomy into the subretinal space. Inserter made by Michael Ault (Synergetics, Inc., O'Fallon, MO).

The PI implants were fabricated by spin coating on silicon wafers, curing, and patterning by photolithography and reactive ion etching (RIE) into a thickness of 10 μm. Amorphous carbon (AC) was deposited using two different techniques: a pulsed laser ablation of a graphite target using a custom-built Neocera instrument and cathodic arc vapor deposition (University of Alabama, Huntsville, AL). An ultra–high-purity graphite crucible served as a cathode, and anhydrous methanol was delivered via a hallow anode, where the plasma was struck. Both processes enabled depositions at ambient temperatures. Pulsed laser ablation was also used. AAO was deposited by argon ion beam chemical vapor deposition. Aluminum was sputtered in the presence of oxygen onto the PI film (Discovery 18; Denton Vacuum Inc., Cherry Hill, NJ). Parylene was deposited onto PI using a parylene coating system (Specialty Coating Systems, Indianapolis, IN). A quantity of dimer was weighed and placed into a heated chamber; this precursor evaporated and diffused into the evacuated deposition chamber, where its vapor condensed simultaneously as parylene onto all surfaces of the parts to be coated. Approximately 2 μm of parylene was physically adsorbed onto the PI test strip surface, where it polymerized. Monothiolated PEG (molecular weight [MW], 5000; Nektar Therapeutics, Inc., San Carlos, CA) was deposited by chemicosorption onto a 1-μm layer of gold that had been adhered to the PI. PVP (MW: 10,000; Sigma-Aldrich) was deposited on PI by physicoadsorption out of a 25% polymer solution in isopropyl alcohol.[12]

The morphologies of surfaces of all the materials (and all the actual implants) was assessed with several techniques, including light microscopy, atomic force microscopy (AFM), and scanning electron microscopy (SEM). For all materials (and all the actual implants), chemical composition was assessed with electron-dispersive spectroscopy. The adhesion of the deposited thin films on the surface of the PI implants was validated and their thicknesses were determined by profilometry and AFM step-height analysis.

The smoothness of our coatings was in the nanometer scale. Before implantation, all materials were observed first on a micrometer scale by SEM, which revealed for all implants a virtually smooth surface (i.e., no trenches or other imperfections) under visible examination at a magnification 500 to 8330×. Then, the smoothness of the coatings was further assessed on a nanometer scale by AFM, which revealed a variation in topology of only 10 to 15 nm. The "Scotch tape test" with visual inspection was used to assess delamination, using large samples (much larger than our implants). With AAO, delamination occurred in

4.7% of the large specimens; however, no obvious delamination occurred in the implant-sized materials. With AC, delamination occurred because of the build-up of internal stress when we studied relatively large areas. Use of a rotating sample holder minimized the problem because the coating could be deposited symmetrically over the substrate, but our implants were too small to be held by the rotating holder. Fortunately, the small size of our implants greatly minimized the internal stress, and no areas of delamination were identified with the Scotch tape test for our AC implants.

On completion of the fabrication or deposition processes, the materials were cleaned and handled according to a protocol in which they were washed in a beaker of warm distilled water and laboratory soap (Fisher FL-70), while the surfaces were swabbed gently with a camel hair brush and then rinsed with acetone followed by isopropyl alcohol, then distilled water, and finally another rinse in isopropyl alcohol. The prepared samples were air-dried on a new glass slide, then placed in a sterilization pouch for ethylene oxide gas sterilization. The pouches were opened within a sterile field at surgery.

Histology

For each animal that had received an implant, 25 slides (each containing four cross sections) were made at equally spaced intervals throughout the region of each implant. The most anatomically well-preserved cross section on each slide was selected for analysis. Thus, 100 cross sections were studied for each material (i.e., 25 cross sections for each of the four implant recipients). All sections were assessed for evidence of inflammation; hemorrhage; outer nuclear layer or inner nuclear layer cell loss or disorganization; Müller cell hypertrophy; continuous or discontinuous reactive tissue and disruption, proliferation, metaplasia or migration of the retinal pigment epithelium (RPE), either above or beneath the implant.

Statistical Analysis

The results of electrophysiological and histologic studies were assessed with paired, two-tailed Student's *t*-tests.

Results

All surgeries were performed without significant complications. In implanted eyes, the foreign materials remained flat and fully extended under the retina, except in two eyes in which an AAO implant curved upward slightly into the retina. Small amounts of bleeding, which occurred intraoperatively at retinotomy sites, resorbed quickly and were not clinically significant. Surgically induced retinal detachments all resolved within the first week. In one pig with a PVP implant, mild inflammation with fibrin formation was observed over the first 2 months, probably secondary to disruption of the crystalline lens during the vitrectomy. Funduscopy at and after the first month showed hypo- and hyperpigmentation of the RPE under the surgically induced retinal detachment in all animals (Fig. 2).

Electrophysiology

In control animals, ERG responses were at or above baseline after surgery. For implanted animals, Figure 3 shows normalized ERG responses at periodic intervals over a 3-month period for each material. One week after surgery, there was a nonstatistically significant reduction in the ERG b-wave with PI, AAO, and parylene. For the other materials, the ERGs were roughly equal to or greater than baseline 1 week after surgery. At the 12th postoperative week, the ERG amplitudes were roughly equal to or greater than baseline for all materials (including AC), without statistically significant differences compared with baseline amplitudes. This conclusion was verified by analyzing the differences over the 3 months, both for the normalized and raw ERG amplitudes (two-tailed Student's *t*-test: $P = 0.2$ and 0.8, respectively).

Histopathology

Histologic results are selectively shown in Figure 4 and summarized across all experiments in Tables 2 and 3. In control

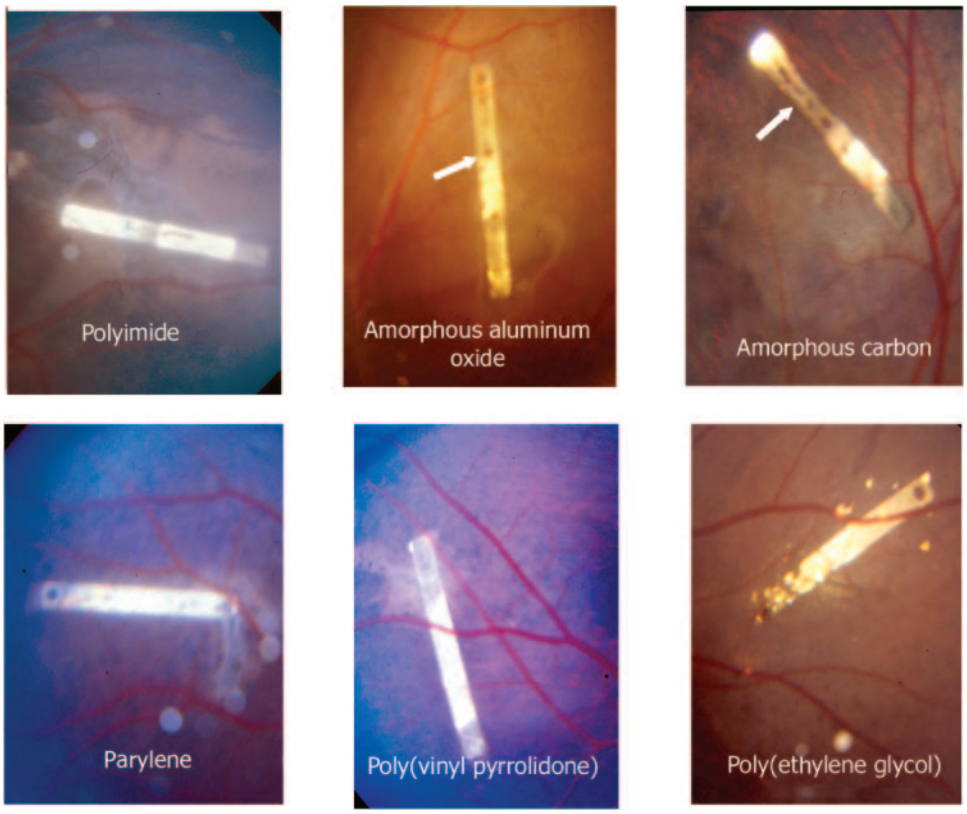

Figure 2. Representative fundus photographs showing examples of each of the six implanted materials 3 months after subretinal implantation in pigs. All retinas remained attached. Migration of RPE cells can be seen on the inner (i.e., vitread facing) side of some implants (*white arrows*).

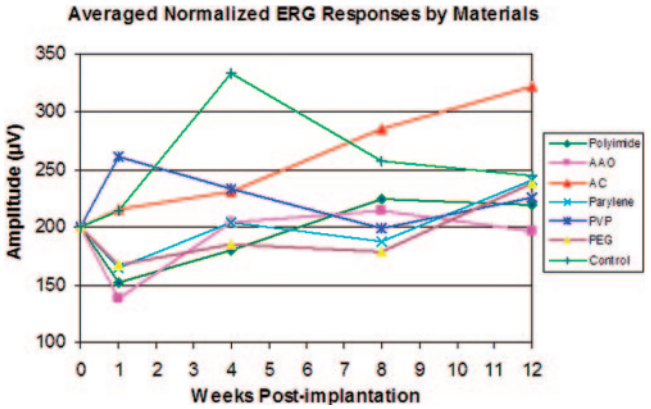

FIGURE 3. Averaged and normalized b-wave amplitudes of the electroretinogram (ERG) taken at regular intervals before and after subretinal implantation in 28 pigs. Each of the 35 data points represents median values obtained from animals that underwent the same type of implant or surgery (i.e., four animals for each implanted material and four animals for "control" experiments in which intraocular surgery was performed but without implanting a foreign material into the subretinal space). For each testing period for each animal, two ERGs were obtained, and the results of each were averaged. A total of 280 ERGs were performed to obtain the data shown on this graph. Each ERG trial consisted of 100 consecutive, computer-averaged stimulations. The results of two trials (i.e., 200 stimulations) were averaged. All baseline values (i.e., those obtained at time point "0", which was just before surgery), were normalized across all animals to a value of 200 μV. All subsequent recordings were graphed as a change proportionate to a starting value of 200. In most animals, there was a reduction of amplitudes at one week after surgery. Thereafter, the ERG amplitudes remained stable or showed recovery to or above baseline. No statistically significant loss of the ERG amplitude was observed at the end of the third postoperative month compared with presurgical amplitudes.

animals, histology revealed only minimal disruption of the normal anatomy. For the control animals, a review of a total of 100 slides (25 slides for each control animal) revealed no inflammation or hemorrhage in any slide; no obvious loss outer nuclear layer (ONL) cells in any sample, although photoreceptor outer segment length was routinely shortened and distorted; no pseudorosette formation in any slides disruption of the RPE monolayer in 4 of 100 samples; metaplasia or proliferation in 9 of 100 samples; RPE migration into the retina in 6 of 100 slides and no subretinal fibrosis in any sample. There was no difference in the histologic results between the two types of control experiments (two-tailed, paired Student's *t*-test that compared the total number of abnormal samples for each type of control experiment: $P = 0.26$).

By comparison, after implantation of each type of material, loss of cells and general disorganization was more evident in the ONL than in the inner nuclear layer (INL). In the ONL, loss of photoreceptors with disorganization was always seen. Loss of fewer than three layers in the ONL was found with all specimens, whereas more significant loss ($\geq$3 layers) was found in 30 of 100, 35 of 100, and 30 of 100 samples of PI, AAO, and AC, respectively. In the INL, disorganization was seen with all materials, especially with AAO and AC. No loss of INL cell layers was observed with parylene, PVP, and PEG. Loss of fewer than three INL layers was found in 18 of 100, 35 of 100, and 20 of 100 slides of PI, AAO, and AC, respectively. Loss of three or more layers of INL cells was not seen with any material. Hemorrhage was not identified in any eye. Inflammation was discovered in only one eye, and this was within the retina at a location considerably removed from the implant. In implanted eyes, there was always some disruption of the normal monolayer organization of the RPE. Proliferation, metaplasia, and migration of the RPE occurred to some extent in all animals implanted with PI, AC, or PEG (vs. two or fewer animals for each of the other materials). In all implanted eyes, the retina away from the implanted area appeared normal.

Results of statistical comparisons between the control experiments versus animals with implanted materials were as follows. Across all variables listed in Table 2, each of the implanted materials produced histologic abnormalities that were significantly greater than that in control animals (Table 3). However, PEG, parylene, and PVP produced relatively less histologic disruption compared to the other three materials (i.e., $<$350 of 1500 abnormal samples each for PEG, parylene, and PVP vs. $>$500 abnormal specimens each for AC, PI, and AAO).

Statistical comparison of outcomes was also performed for each major heading shown in Table 2. In the analysis of retinal disease, parylene and PEG did not show a significant difference in outcome versus the control animals, whereas the other four materials produced statistically significant differences compared with the control animals. Parylene produced significantly fewer histologic alterations of the retina than did AAO, AC, or PI. PEG produced significantly fewer histologic alteration of the retina than did PI (the results of the comparison to AAO nearly reached statistical significance: *t*-test = 0.06). There were no other statistically significant differences among the materials with respect to the analysis of retinal pathology.

For the analysis of RPE responses, PI and AAO produced histologic alterations that were significantly greater than those in the control animals ($P = 0.03$ and 0.009, respectively), but the other four materials did not differ from the control subjects in the extent to which they produced alterations of the RPE. Parylene, PEG, and PVP, the best three performing materials in this domain, produced significantly less RPE reaction than did PI or AAO, but did not differ significantly from AC. In contrast, AC did not differ from results with either PI or AAO.

For the analysis of cellular responses surrounding the implant, there was a clearer bimodal distribution of results among the materials AC, PEG, PVP, and parylene, which did not differ from one another. All produced significantly fewer cellular responses surrounding the implant than did AAO or PI. The latter two materials did not differ from one another in their tendency to incite cellular responses around the implant.

DISCUSSION

Epi- and subretinal microelectronic implants are being developed as prosthetic devices.[1,4,13–15] In either case, the device must be placed near the retina for efficient activation of neurons. The biocompatibility of materials on each surface of the retina is likely to be different because of relative differences in tissue responses and surgical trauma for each approach and the need to attach implants to the epiretinal surface. Our implant is designed for the subretinal space; hence, our methods reflect this approach.

Previous Studies of the Biocompatibility of Retinal Implants

The biocompatibility of retinal implants has been studied by several groups that have used either the epi- or subretinal means of implantation. On the epiretinal side, three studies have examined to some extent the reactions to chronic implantation of an electrode array. Walter et al.[5] implanted two types of arrays, one of which was microfabricated and the other of which was made of silicone. Both were implanted after vitrectomy and laser photocoagulation, and retinal tacks were used to fixate the devices. Six months after implantation, "no change in retinal architecture underneath the implant was

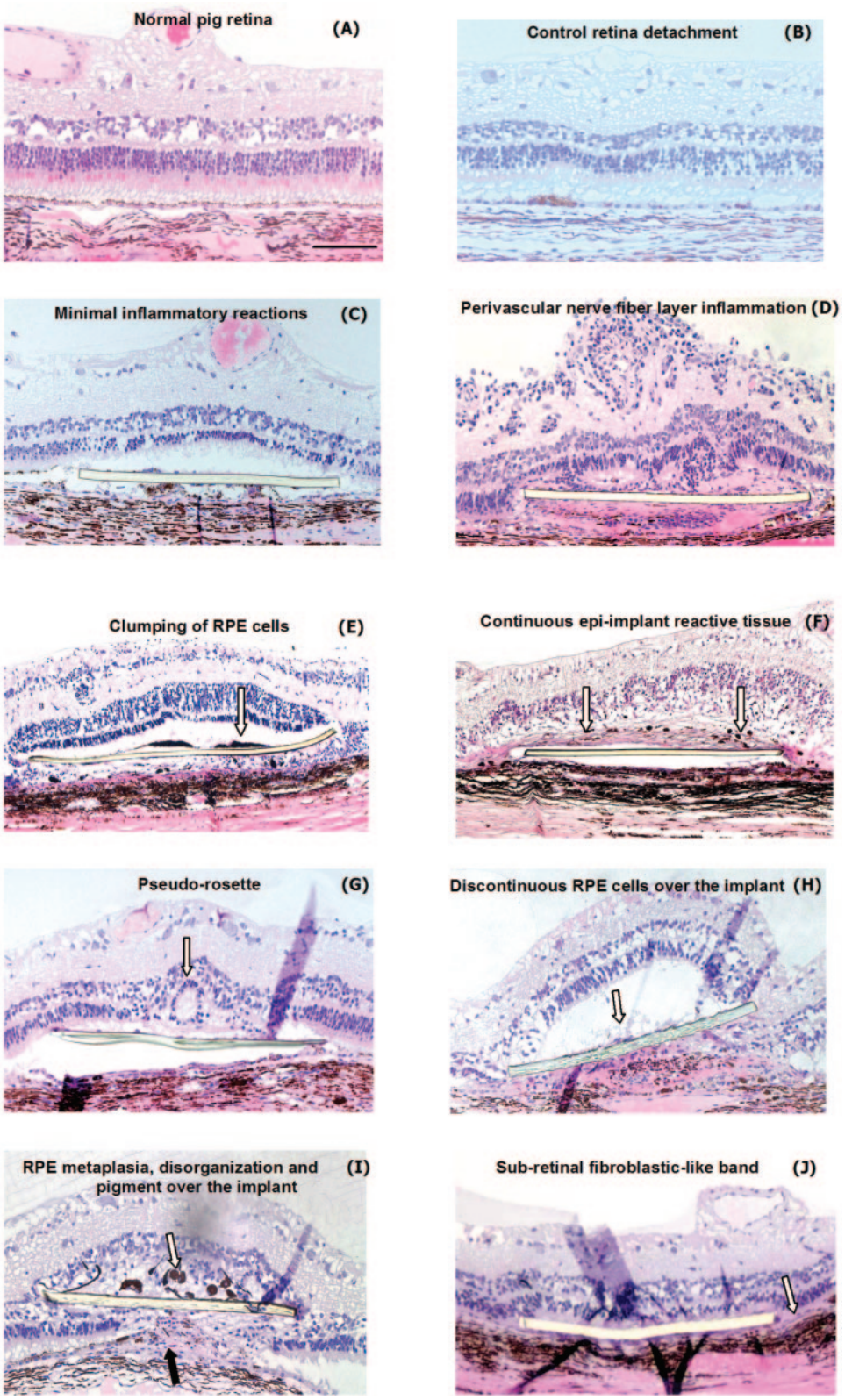

FIGURE 4. Selected histology of pig retinas. (**A**) Normal pig retina. (**B**) Retina 3 months after a "control" surgery in which a retinotomy and retinal detachment were made without implantation. Various types of tissue reactions 3 months after subretinal implantation of six different, nonelectronic implants through a retinotomy (**C**–**J**). (**C**) Relatively little anatomic alteration after implantation of parylene; (**D**) perivascular nerve fiber layer inflammation and gross irregularity after implantation with poly(vinyl pyrrolidone); (**E**) example of clumping of RPE cells over the implant, after implantation with PI; (**F**) continuous epi-implant reactive tissue around the implant after implantation with PI; (**G**) pseudorosette formation within the retina overlying the implant, after implantation with AAO; (**H**) discontinuous RPE cells overlying the implant after implantation with amorphous carbon; (**I**) clumping (*white arrow*), disorganization, and metaplasia (*black arrow*) of the RPE cells under the implant, after implantation of PEG. RPE cells separated from Bruch's membrane and migrated over the implant; (**J**) subretinal fibroblastlike band, after implantation of PEG. All implants were made as 0.5 × 5.0-mm strips that were 10 μm thick, and all were implanted through a retinotomy. Hematoxylin and eosin staining in all examples. Final magnification, ×20. Scale bar, shown in **A**, equals 100 μm and is applicable to all photographs in this figure.

found by light microscopy" in 10 rabbits, although the one photomicrograph that was provided revealed significant compression of the retina. One retinal detachment occurred.

The second epiretinal study was performed by implanting nonmicrofabricated, ≈1-mm-thick silicone slabs with 25 embedded platinum wires, which were implanted in four dogs after vitrectomy. Two metal alloy tacks were used to secure the array to the retina. "Total preservation of the retina underlying the electrode array," which seemed evident in the one photomicrograph provided, was reported.[6] However, it is not possible to ascertain whether the array was in contact with the retina in the area from which the photomicrograph was made. A sheet of relatively thick silicone would not likely fully conform to the retinal surface; hence, it seems likely that some

TABLE 2. Overview of Histologic Results from All Materials and All Animals

	Control ($N = 4$)	AAO ($N = 4$)	Polyimide ($N = 4$)	AC ($N = 4$)	PVP ($N = 4$)	Parylene ($N = 4$)	PEG ($N = 4$)
Retinal pathology							
Inflammation	0/100	0/100	0/100	0/100	25/100(1)	0/100	0/100
Hemorrhage	0/100	0/100	0/100	0/100	0/100	0/100	0/100
ONL cell loss	11/100(4)	35/100(4)	30/100(4)	30/100(4)	10/100(1)	**0/100**	**0/100**
(≥3 cell layers lost)	3 [1]	9 [2]	6 [6]	8 [3]			
INL cell loss	0/100	35/100(3)	18/100(4)	20/100(4)	**0/100**	**0/100**	**0/100**
(<3 cell layers lost)		12 [2]	4 [2]	4 [3]			
ONL disorganization	30/100(4)	100/100	100/100	100/100	100/100	100/100	100/100
	8 [1]						
INL disorganization	0/100	84/100(4)	70/100(4)	80/100(4)	**25/100**(4)	40/100(4)	40/100(3)
		20 [4]	18 [5]	20 [1]	5 [3]	9 [3]	15 [3]
Müller cell hypertrophy	0/100	25/100(4)	40/100(4)	35/100(4)	25/100(4)	**20/100**(4)	25/100(4)
		7 [1]	10 [2]	8 [5]	5 [3]	5 [1]	7 [2]
Pseudo-rosettes in ONL	0/100	90/100(4)	15/100(4)	80/100(4)	20/100(2)	**0/100**	**0/100***
		23 [3]	4 [1]	20 [4]	10 [7]		
Retinal pigment epithelium							
Disruption of the normal	32/100(4)	75/100(4)	75/100(4)	60/100(4)	65/100(4)	60/100(4)	**40/100**(4)
monolayer of the RPE	9 [2]	16 [4]	19 [6]	18 [7]	16 [7]	15 [11]	10 [2]
Metaplasia and RPE	13/100(4)	40/100(4)	65/100(4)	22/100(4)	10/100(4)	**0/100**	15/100(4)
proliferation†	2 [4]	10 [2]	16 [6]	5 [4]	3 [1]		3 [3]
RPE migration†	10/100(4)	40/100(2)	35/100(4)	28/100(4)	**10/100**(1)	15/100(2)	25/100(4)
	2 [3]	20 [3]	9 [1]	7 [5]		7 [1]	5 [4]
Cellular responses surrounding the implant							
Continuous layer of epi-implant-reactive tissue							
< 10 μm thickness	—	35/100(2)	25/100(2)	**0/100**	20/100(1)	5/100(1)	**0/100**
		18 [10]	13 [3]				
≥10 μm thickness	—	10/100(1)	10/100(1)	**0/100**	**0/100**	**0/100**	**0/100**
Continuous layer of subimplant-reactive tissue							
< 10 μm thickness	—	28/100(2)	12/100(1)	**0/100**	20/100(1)	5/100(1)	10/100(1)
		14 [13]					
≥10 μm thickness	—	**0/100**	4/100(1)	**0/100**	**0/100**	**0/100**	**0/100**
Discontinuous layer of epi-implant cells (total nuclei)							
< 5 cells	—	35/100(4)	45/100(4)	30/100(4)	**5/100**(4)	20/100(4)	10/100(4)
		10 [3]	13 [7]	9 [2]	1 [1]	5 [5]	2 [1]
≥5 cells	—	10/100(4)	15/100(4)	10/100(4)	**0/100**	12/100(4)	10/100(4)
		3 [1]	3 [2]	2 [1]		3 [1]	2 [1]
Discontinuous layer of subimplant cells (total nuclei)							
< 5 cells	—	50/100(4)	15/100(4)	**0/100**	**0/100**	20/100(4)	15/100(4)
		13 [3]	3 [2]			5 [2]	4 [2]
≥5 cells	—	24/100(4)	14/100(4)	15/100(4)	12/100(4)	**10/100(4)**	**10/100(4)**
		6 [1]	3 [2]	4 [2]	3 [1]	**3 [1]**	**2 [1]**

The materials are listed in descending order of the number of abnormal slides across all variables (see Table 3 for quantitative summary). No values are listed in the first column for the controls under the heading "cellular responses surrounding the implant" because the control experiments did not include an implant. Bold data indicate which material fared best for each variable. Values in parenthesis indicate the number of animals in which a particular histologic feature was identified. The bottom line within each data block provides the median and [standard deviation] for instances in which more than one animal demonstrated a histologic abnormality for that variable. "Müller cell hypertrophy" was scored when there was obvious thickening of >2 Müller cell profiles in a given cross section. AAO, amorphous aluminum oxide; AC, amorphous carbon; PVP, poly(vinyl pyrrolidone); PEG, poly(ethylene glycol).

* There was one case of pseudorosette formation away from the implant.

† Our ability to define these changes depended upon identifying melanin pigment granules. As such, it is possible that some changes of this type may have escaped our detection if the cells did not show pigment granules in the sections that we studied.

portion of the array may have vaulted over the retina. The challenge of obtaining a conformal alignment along the retina apparently produced retinal compression in some eyes.[6] Another study by the same group assessed the gross effects of epiretinal implantation of poly(dimethyl siloxane) electrode arrays in dogs. Similar favorable conclusions were drawn from this work, but like the former study, a detailed and quantitative histologic assessment is not provided.[11] In the latter study, the use of optical coherence tomography provided a realistic appreciation of the proximity of the array to the retina, and some gliosis and loss of neurons was appreciated at locations where the array compressed or at least contacted the retina.

On the subretinal side, Peyman et al.[7] were the first to report the results of chronic implantation. Rabbits were implanted with 250-μm-thick silicon microphotodiode arrays in an intravitreal approach. They reported fibrosis over some

TABLE 3. Statistical Comparison of the Histologic Results of the Control Animals versus Each Implanted Material

Controls or Implanted Materials ($n = 4$ for each)	Number of Slides with Abnormalities	Statistical Significance: Materials versus Controls (Student Paired *t*-Test)
Controls	96/1100	
AAO	697/1500	$P = 0.00005$
Polyimide	588/1500	$P = 0.00004$
AC	515/1500	$P = 0.002$
PVP	347/1500	$P = 0.005$
Parylene	307/1500	$P = 0.022$
PEG	300/1500	$P = 0.019$

The control experiments did not include an analysis of histologic features under the heading "cellular responses surrounding the implant" (see Table 2) because the control experiments did not include an implant. Hence, only 1100 slides were assessed for the four control animals versus the 1500 that were assessed for the animals that had received an implant. The number of "abnormalities" listed in the second column is the total number of histologic abnormalities for the control studies or each of the materials, as can be extracted from Table 2. AAO, amorphous aluminum oxide; AC, amorphous carbon; PVP, poly(vinyl pyrrolidone); PEG, poly(ethylene glycol).

devices, and "significant loss of retinal cells in areas overlying the implant." There was significant full-thickness disruption of the retina, especially the outer retina. This is not unexpected, given that rabbits do not have a retinal circulation and are therefore entirely dependent on choroidal diffusion for nutrients, which is likely disrupted by the subretinal, nonperforated device. Peyman et al.[7] do not indicate how many animals received implants, and, in the only photomicrograph provided, there is no indication of survival time.

A subsequent study by the same group was performed by implanting electrically active or inactive silicon discs into 10 cats. The longest surviving animal, which had received an electrically inactive device, exhibited marked loss of photoreceptors only. The relative sparing of the inner retina, although with some disorganization, is expected, given the presence of retinal circulation in this species. The electrically active devices were 2.0- to 2.5-mm diameter, 50-μm-thick, silicon photodiodes with gold electrodes. These implants produced a 10% to 15% reduction in the ERG b-wave amplitudes. RPE changes were seen at the surgical site, but not elsewhere. Overlying the implant, there was a marked loss of photoreceptors, and the "architectural arrangement of the inner layers was somewhat disorganized." Cell counts in the INL and RGC layers were not significantly different from areas away from the implant or from controls.[8]

As an extension of this group's work, Pardue et al.[9] did more extensive histologic and immunohistochemical analyses of the feline retinas implanted with subretinal arrays. Similar changes were noted in the outer retina. The inner retina over the implant was relatively intact, but there was some disorganization of the INL, with cell loss over the center of the implant. There was an inflammatory response around the implants, with giant cell reactions. Müller cells over the implant had increased expression of glial fibrillary acidic protein (GFAP), but the retina adjacent to the implant showed a normal distribution of GFAP in astrocytes. In general, glutamate staining was decreased, but not in the inner retina. GABA labeling was reduced over the implant, as was the number of horizontal cells. Pardue et al.[9] concluded that the inner retinal changes were most likely secondary to degeneration of the outer retina that had been induced by the separation of the outer retina from its choroidal nutrition by the implant.

Another subretinal study by Zrenner[13] inserted silicon microphotodiode arrays with titanium nitride (TiN) electrodes in the subretinal space of rats via an ab externo technique. In general, they found changes similar to those found by Peyman et al.[7] in the outer retina. The thickness of the INL, however, was normal. Müller cells showed enhanced GFAP labeling, and there was an increased number of cells in the ganglion cell layer, which they attributed to an astrocytic reaction. Given that degeneration of the outer retina was most severe over the center of implants, Zrenner[13] proposed using perforated devices to allow more diffusion of nutrients to the retina.

Our Study of Biocompatibility

Our study differs from the earlier works in that we (1) surveyed a selection of candidate materials for a retinal prosthesis (Table 1) across a relatively large number of animals; (2) assessed a large number (i.e., 15) of histologic criteria; (3) obtained a large representation of histology (i.e., 100 slides for each material); (4) provide a statistical analysis of outcomes; and (5) performed control experiments. Using these methods, we found (1) that all implants generally produced more disruption of the retina or RPE than cellular responses surrounding the implant; (2) generally, there were more well-preserved nuclear cells in the inner than the outer retina over the implants, and retinas were normal distant from all implants; (3) there were few instances of "continuous" reactive tissue covering the implants; and (4) there was only one retina with histologic evidence of inflammation. Overall, PEG, parylene, and PVP performed best across all the histologic measures that were studied (Table 3).

We found in all specimens disorganization of the ONL and some loss of the photoreceptor cells, which is to be expected, given the fact that the subretinal, nonperforated implants would have compromised nourishment to the outer retina in this porcine model. Our choice of pigs, however, has the advantage that we were able to study the health of the inner retina after implantation more reasonably, because pigs have both choroidal and retinal arterial blood supply to the retina, unlike rabbits, for instance. The eyes of pigs are also advantageous because they are similar in size to those of humans, which facilitates development of the mechanical design of our prosthesis. Porcine eyes are also less prone than rabbits' eyes to ocular inflammation. Our electrophysiological assessment of the implanted animals revealed a temporary postoperative decrease of the ERG, with recovery to normal within 1 month after implantation. The induced retinal detachment and performance of a vitrectomy alone, and not the presence of the implanted materials, could account for the decline in ERG amplitudes.[15–18]

Some more specific comments about our histology are relevant to the interpretation of our results. The one histologic specimen with inflammation was obtained from an animal that experienced persistent and clinically evident postoperative inflammation within the eye. The inflammatory cells were present only in the INL, and thus were not adjacent to the implant, and such cells were also found distant from the implant. These findings suggest that the inflammation was not related to the material. It is possible that the process of making the retinal detachment might have produced some of the pathologic conditions we observed. Other studies and our own control animals from this study have shown that creation of a retinal bleb can liberate RPE cells, damage Bruch's membrane and generally cause disease in the outer retina, even with relatively brief detachments lasting only days.[19–23] Subretinal gliosis, similar to that which we found around our implants,

and growth of Müller cell processes into the subretinal space is a relatively common occurrence after retinal reattachment in cat.[24] As such, it is likely that some of the changes we observed with implants are related to the surgery itself. The anticipation that surgically induced disease might confound our attempts to study the of biocompatibility of the materials prompted us to use surgical techniques that would minimize the amount of surgery needed to implant the materials and which could be performed with a high degree of reliability. In fact, we did not begin this study until we had demonstrated a high success rate, which accounts for our ability to perform 26 of 26 surgeries without significant complications, notwithstanding the one case with postoperative inflammation.

There were some individual differences among the materials with respect to the degree that they altered the normal anatomy of the retina or the RPE or the degree to which they incited reactions around the implant itself. With respect to the alterations induced within the retina, parylene, and PEG did not show any significant difference in outcome versus the control animals, whereas the other four materials produced statistically significant differences compared with the control animals. Parylene produced significantly fewer histologic alterations of the retina than AAO, AC, or PI. PEG produced significantly fewer histologic alterations of the retina than PI. In general, with our subretinal implants, we found seemingly less outer retinal degeneration than Peyman et al.[7] and Zrenner,[13] perhaps because we studied different materials that were also thinner than those used by the others.

With respect to the induction of RPE reactions, only PI and AAO produced histologic alterations that were significantly greater than those in the control animals. Parylene, PEG and PVP produced the fewest RPE reactions. With respect to the formation of cellular responses around the implant, AC, PEG, PVP, and parylene all fared better than either AAO or PI. We found it remarkable that, around these better performing materials, there was almost no "continuous" tissue reaction of the type that would raise serious concerns about potential hindrance of electrical output from a stimulating array made of these materials.

Our current methods of obtaining a relatively large number of histologic sections throughout the area of the implant provide a good perspective on which materials are generally more biocompatible. The results of our screening analyses can be enhanced in future studies by incorporating immunohistochemistry or electron microscopy of the more promising materials. The choice of materials for the more detailed studies will be influenced not only by the results of this study but also by results of "electrical soak" tests that are being performed to analyze the resilience of these materials as electrical insulators when maintained chronically in salt water, which is a mandatory property for a chronically implanted, electrically active device such as a prosthesis. This base of knowledge of biological damage induced by the materials themselves is a necessary prerequisite for subsequent studies regarding any superimposed damage that might be induced by electrical stimulation of chronically implanted devices.

In summary, some degree of biological disruption secondary to surgery and physical implantation of a foreign material under or on top of the retina is probably unavoidable. Hence, our goal is to develop minimally invasive surgical techniques and to use materials and a prosthetic design that will minimize tissue reactions. Overall, we found that PEG, parylene, and PVP produced the least disruption of the normal tissues after 3 months of implantation into the subretinal space of pigs. However, all implants produced some alteration of the retina, but this study does not address whether this degree of biological reaction would be detrimental to the responsiveness of the retina to prosthetic stimulation. This study also does not provide insight into reactions that may occur over longer periods, especially if the materials degrade within the saline environment of the eye or in response to delivery of electrical currents. Nonetheless, our results indicate that the biological reactions to the surgery and materials that we used were relatively mild and somewhat encouraging with respect to their potential use in a retinal prosthesis.

Acknowledgments

The authors thank Thaddeus Dryja, MD, for assistance in the interpretation of the pathologic responses of the retina and retinal pigment epithelium after surgery and implantation; Jinghua Chen, MD, for assistance in some of the surgeries; and Tong-Zhen Zhao, MD, for assistance in preparing the histologic slides.

References

1. Loewenstein JI, Montezuma SR, Rizzo JF. Outer retinal degeneration: an electronic retinal prosthesis as a treatment strategy. *Arch Ophthalmol*. 2004;122:587–596.
2. Rizzo JF, Wyatt J, Loewenstein J, et al. Perceptual efficacy of electrical stimulation of human retina with a microelectrode array during short-term surgical trials. *Invest Ophthalmol Vis Sci*. 2003; 44:5362–5369.
3. Rizzo JF, Wyatt J, Loewenstein J, et al. Methods and perceptual thresholds for short-term electrical stimulation of human retina with microelectrode arrays. *Invest Ophthalmol Vis Sci*. 2003;44: 5355–5361.
4. Rizzo JF, Wyatt J, Humayun M, et al. Retinal prosthesis: an encouraging first decade with major challenges ahead. *Ophthalmology*. 2001;108:13–14.
5. Walter P, Szurman P, Vobig M, et al. Successful long-term implantation of electrically inactive epiretinal microelectrode arrays in rabbits. *Retina*. 1999;19:546–552.
6. Majji AB, Humayun MS, Weiland JD, et al. Long-term histological and electrophysiological results of an inactive epiretinal electrode array implantation in dogs. *Invest Ophthalmol Vis Sci*. 1999;40: 2073–2081.
7. Peyman G, Chow AY, Liang C, et al. Subretinal semiconductor microphotodiode array. *Ophthalmic Surg Lasers*. 1998;29:234–241.
8. Chow AY, Pardue MT, Chow VY, et al. Implantation of silicon chip microphotodiode arrays into the cat subretinal space. *IEEE Trans Neural Syst Rehabil Eng*. 2001;9:86–95.
9. Pardue MT, Stubbs EB, Perlman JI, et al. Immunohistochemical studies of the retina following long-term implantation with subretinal microphotodiode arrays. *Exp Eye Res*. 2001;73:333–343.
10. Xiao X, Wang J, Liu C, et al. In vitro and in vivo evaluation of ultrananocrystalline diamond for coating of implantable retinal microchips. *J Biomed Mater Res B Appl Biomater.* 2006;77:273–21.
11. Guven D, Weiland J, Maghribi M, et al. Implantation of an inactive epiretinal poly(dimethyl siloxane) electrode array in dogs. *Exp Eye Res*. 2006;82:81–90.
12. Sweitzer R, Scholz D, Montezuma S, Rizzo JF. Evaluation of subretinal implants coated with amorphous aluminum oxide and diamond-like carbon. *J Bioact Compat Polymers*. 2006;21:5–22.
13. Zrenner E. *Are Subretinal Microphotodiodes Suitable As a Replacement for Degenerated Photoreceptors?* New York: Kluwer Academic/Plenum; 1999.
14. Weiland JD, Liu W, Humayun MS. Retinal prosthesis. *Annu Rev Biomed Eng,*. 2005;7:361–401.
15. Miyake Y, Yagasaki K, Horiguchi M. Electroretinographic monitoring of retinal function during eye surgery. *Arch Ophthalmol*. 1991;109:1123–1126.
16. Miyake Y, Horiguchi M. Electroretinographic alterations during vitrectomy in human eyes. *Graefes Arch Clin Exp Ophthalmol*. 1998;236:13–17.

17. Horiguchi M, Miyake Y. Effect of temperature on electroretinograph readings during closed vitrectomy in humans. *Arch Ophthalmol*. 1991;109:1127–1129.
18. Montezuma S, Rizzo JF, Ziv O. Differential recovery of the ERG, VECP and EECP following vitrectomy: implications for acute testing of an implanted retinal prosthesis. *J Rehabil Res Devel*. 2004; 41:113–120.
19. Kroll AJ, Machemer R. Experimental retinal detachment in the owl monkey. 3. Electron microscopy of retina and pigment epithelium. *Am J Ophthalmol*. 1968;66:410–427.
20. Erickson PA, Fisher SK, Anderson DH, et al. Retinal detachment in the cat: the outer nuclear and outer plexiform layers. *Invest Ophthalmol Vis Sci*. 1983;24:927–942.
21. Anderson DH, Stern WH, Fisher SK, et al. Retinal detachment in the cat: the pigment epithelial-photoreceptor interface. *Invest Ophthalmol Vis Sci*. 1983;24:906–926.
22. Anderson DH, Guerin CJ, Erickson PA, et al. Morphological recovery in the reattached retina. *Invest Ophthalmol Vis Sci*. 1986;27: 168–183.
23. Guerin CJ, Anderson DH, Fariss RN, Fisher SK. Retinal reattachment of the primate macula; photoreceptor recovery after short-term detachment. *Invest Ophthalmol Vis Sci*. 1989;30: 1708–1725.
24. Lewis GP, Fisher SK. Müller cell outgrowth after retinal detachment: association with cone photoreceptors. *Invest Ophthalmol Vis Sci*. 2000;41:1542–1545.